Nucl. Phys. B 1018 (2025) 117069

Contents lists available at ScienceDirect

Nuclear Physics, Section B

journal homepage: www.elsevier.com/locate/nuclphysb

Particle Cosmology

Impact of dark matter halo on black hole: Thermodynamical properties and photons motion

Abdelhakim Benkrane *, Djamel Eddine Zenkhri

Université Kasdi Merbah Ouargla, Laboratoire LRPPS, Ouargla 30000, Algeria

ARTICLE INFO

Editor: Yasaman Farzan

Keywords:
DM halo
Thermodynamical properties
Dehnen-type profile
Schwarzschild BH
BH shadow
Energy emission rate

ABSTRACT

This paper investigates the thermodynamic properties of a Schwarzschild black hole (BH) surrounded by a dark matter (DM) halo, modeled using a Dehnen-type density profile. Specifically, we analyze the influence of the halo's core density ρ_s and scale radius r_s on key thermodynamic quantities, including the black hole's mass, temperature, heat capacity, entropy, and Gibbs free energy. Our results show that the presence of dark matter introduces notable modifications to the black hole's thermodynamics while preserving the fundamental entropy-area relation. Additionally, we examine the effects of the DM halo on the radius of circular photon orbits, the black hole's shadow radius, and the energy emission rate.

1. Introduction

The universe hosts massive astrophysical objects, such as BHs, which play fundamental roles in Einstein's general relativity and alternative theories of gravity. Given their significant gravitational influence, the notion that BHs exist in complete isolation is highly implausible. Instead, they are likely embedded within complex and dynamic environments. For instance, substantial observational evidence supports the hypothesis that supermassive BHs serve as the primary engines driving active galactic nuclei (AGNs) [1,2]. Observational evidence strongly suggests that DM forms halos around most galaxies [3] and influences cosmic structures. Galactic rotation curves support its presence [4], bullet cluster dynamics [5], baryon acoustic oscillations, and cosmic microwave background (CMB) measurements [6]. CMB data further indicate that the Universe is predominantly composed of DM ($\sim 27\%$, which is equivalent to 85% of the total mass of the universe [7]) and dark energy ($\sim 68\%$). In the early universe, the DM halo has been proposed as a key factor in explaining this phenomenon. A coherent explanation for these observations is challenging without postulating a substantial presence of DM in the universe.

A wide range of DM halo models have been proposed, drawing from both simulation results and astrophysical observations. Several BH (BH) solutions have also been explored, including those incorporating a DM profile linked to a phantom scalar field [8]. Extensive analyses have provided valuable insights into the characteristics of DM distributions [9–13], while analytical models have been developed to describe supermassive BHs embedded within DM halos [14–16]. Notable DM halo models include the Navarro-Frenk-White [17], Einasto [18,19], Burkert [20], and Dehnen [21] models. Recently, there has been growing interest in the effects of Dehnen-type DM halos on BHs, examined from multiple perspectives. For instance, Ref. [22] investigates how density profile slope variations influence star clusters' survival with low star-formation efficiency following rapid gas expulsion. In addition, the authors of

* Corresponding author.
E-mail addresses: abdelhakim.benkrane@univ-ouargla.dz, hakim9502.benkrane@gmail.com (A. Benkrane), dzenkhri@univ-ouargla.dz (D.E. Zenkhri).

https://doi.org/10.1016/j.nuclphysb.2025.117069
Received 2 May 2025; Received in revised form 7 July 2025; Accepted 4 August 2025

Available online 8 August 2025

Ref. [23] studied the effect of core density and core radius of the DM halo with a Dehnert-type density distribution in the surrounding environment of a Schwarzschild-like BH.

For the sake of transparency, the DM research community is increasingly facing a sense of crisis due to the persistent lack of experimental evidence for leading candidates, including weakly interacting massive particles (WIMPs), axions, and sterile neutrinos, despite extensive and sustained efforts dedicated to their detection. Despite these problems, the authors in Ref. [3] suggest that broadening experimental approaches by integrating astronomical surveys and gravitational wave observations offer the best opportunity for advancing our understanding of the DM problem.

On the other hand, thermodynamics and BHs are deeply related, starting from prior works of Bekenstein and Hawking, where Bekenstein first established a link between a black hole's event horizon area and entropy, noting that both increase irreversibly in classical black holes [24,25]. Later, Hawking introduced quantum effects, revealing that black holes emit radiation, which enables the event horizon area to shrink over time [26,27]. Building on their work and the inspiration they provided to subsequent researchers, the four laws of black hole thermodynamics were formulated [28–30]. All of these factors played a crucial role in forging a strong relationship between thermodynamics and gravity. This connection deepened further with Verlinde's work, published in 2010, where he proposed that gravity is an entropic force [31]. Consequently, numerous scientific studies have examined different aspects of gravity from this perspective [32–35]. However, for the sake of clarity, it is essential to recognize that Verlinde's model, like other theories, encounters both theoretical and experimental challenges and criticisms [36,37].

Our goal in this work is to investigate the impact of a Dehnen-type DM halo on the thermodynamics of a black hole. Additionally, we aim to derive its influence on photon circular motion. In this context, readers must note that the Dehnen density profile [21,38] is often studied in dwarf galaxies, which typically lack central black holes (BHs). However, recent observations suggest that massive BHs may exist in these galaxies. For example, an SMBH of about $2.00\times10^5 M_\odot$ was detected in Mrk 462 [39], while Henize 2-10 hosts an SMBH of approximately $1.00\times10^6 M_\odot$. Additionally, a study on dark matter dynamics found a BH in Leo I, with a mass of $3.3\pm2\times10^6 M_\odot$, making up 13% This paper is structured as follows: Section 2 explores the thermodynamic properties of a black hole surrounded by a DM halo, highlighting the effects of the halo's central density and radius. In Section 3, we study how the effective potential of photons and their circular motion are influenced by the presence of the DM halo. Then, in section 4, we study the impact of DM halo on BH shadow and energy emission rate. Finally, we present our conclusions in Section 5.

2. Thermodynamical properties of Schwarzschild BH in galaxies surrounded by a DM halo

The mass distribution in terms of density profile $\rho(r)$ is given as,

$$M_D = 4\pi \int_0^r \rho(r')(r')^2 dr'. \tag{1}$$

The density of the Dehnen-type DM halo is a special case of a double power-law profile given by

$$\rho(r) = \rho_s \left(\frac{r}{r_s}\right)^{-\gamma} \left[\left(\frac{r}{r_s}+1\right)\right]^{\dfrac{\gamma-\beta}{\alpha}}, \tag{2}$$

where $(\alpha,\beta,\gamma)=(1,4,\gamma)$ [38]. Here, ρ_s and r_s represent the central halo density and radius, respectively, while γ defines the specific variant of the profile. The parameter γ ranges from 0 to 3, with $\gamma=\frac{3}{2}$ commonly used to fit the surface brightness profiles of elliptical galaxies, closely resembling the de Vaucouleurs $r^{1/4}$ profile [38]. Also, this model is especially valuable due to its analytically tractable properties, making it a powerful tool for studying celestial objects. These include the intrinsic velocity dispersion for all real values of γ between 0 and 3, and, for $\gamma=0,1,$ and 2, the projected mass density and velocity dispersion as well [21,40]. The authors in the paper [39] study the impact of DM halo on thermodynamical BH properties using the following parameter $(\alpha,\beta,\gamma)=(1,4,0)$, while in the Ref. [41], Dehnen-type DM halo was used to improve constraints from ultra-faint dwarf galaxies on primordial black holes as dark matter. Following the approach of the authors in Ref. [23], we employ the Dehnen dark matter (DM) halo with parameters $(\alpha,\beta,\gamma)=(1,4,5/2)$. Therefore, Eq. (2) becomes

$$\rho(r) = \frac{\rho_s}{\left(\frac{r}{r_s}\right)^{5/2}\left(\frac{r}{r_s}+1\right)^{3/2}}. \tag{3}$$

If we take into account the pure matter present in BH space-time, represented by the energy-momentum tensor $T_{\mu\nu}(BH)$, alongside the Dehnen-type DM halo spacetime, described by $T_{\mu\nu}(D)$, the Einstein field equation becomes

$$R_{\mu\nu} - \frac{1}{2}Rg_{\mu\nu} = 8\pi\left(T_{\mu\nu}(BH)+T_{\mu\nu}(D)\right). \tag{4}$$

$R_{\mu\nu}$, R, and g_μ are the Ricci tensor, Ricci scalar, and metric tensor, respectively. Here's a more precise rewording:

By solving Einstein's field equations for a pure dark matter (DM) halo and assuming that ρ_s and r_s are sufficiently small, the lapse function $A(r)$ for the pure DM halo can be expanded as follows [23]:

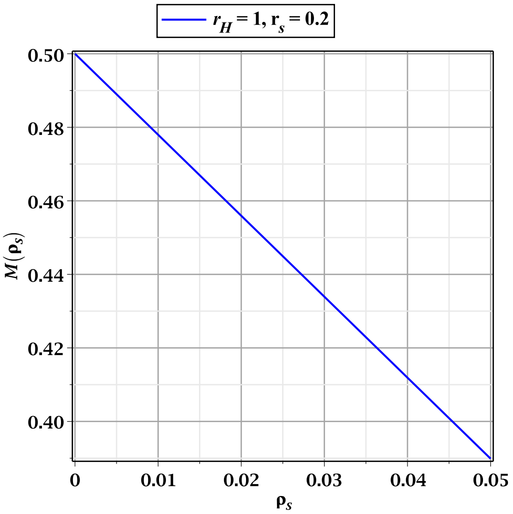

Fig. 1. The impact of central halo density on BH mass. The other parameters are $r_s = 0.2, r_H = 1$.

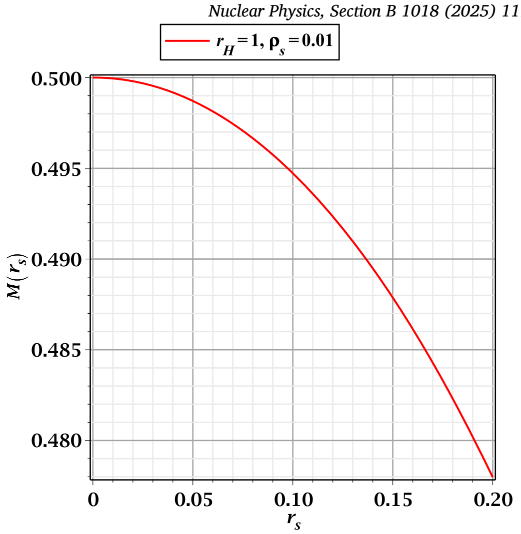

Fig. 2. The impact of central halo radius on BH mass. The other parameters are $\rho_s = 0.01, r_H = 1$.

$$A(r) = \exp\left(-32\pi\rho_s r_s \sqrt{\frac{r + r_s}{r r_s}}\right) \simeq 1 - 32\pi\rho_s r_s \sqrt{\frac{r + r_s}{r r_s}}, \tag{5}$$

where the approximation holds to first order in $\rho_s r_s$. By taking Schwarzschild BH as the boundary condition, one can write the solution of Einstein's field equations (4) metric of the BH space-time combined with DM halo, the space-time metric is given as [23]:

$$ds^2 = -f(r)dt^2 + \frac{dr^2}{f(r)} + r^2 d\theta^2 + r^2 \sin^2\theta \, d\phi^2, \tag{6}$$

where the lapse function is written as

$$f(r) = 1 - \frac{2M}{r} - 32\pi\rho_s r_s^3 \sqrt{\frac{r + r_s}{r_s^2 r}}. \tag{7}$$

The BH mass as a function of event horizon radius r_H, and core density ρ_s and radius r_s can be extracted by $f(r_H) = 0$, therefore

$$M(r_H) = \frac{r_H}{2}\left[1 - 32\pi\rho_s r_s^2 \sqrt{\frac{r_H + r_s}{r_H}}\right]. \tag{8}$$

While the Hawking temperature is determined by the derivation of the lapse function $f(r)$ with respect to r at $r = r_H$, by the following form

$$T(r_H) = \frac{f'(r)|_{r=r_H}}{4\pi}, \tag{9}$$

using the lapse function (7) and the mass of studied BH (8), one can easily show that

$$T(r_H) = \frac{1}{4\pi r_H}\left[1 - 16\pi\rho r_s^2 \frac{2r_H + r_s}{\sqrt{r_H(r_H + r_s)}}\right]. \tag{10}$$

To avoid the non-physical values of temperature and mass, the following condition is required

$$\rho_s \leq \frac{1}{16\pi r_s^2}\sqrt{\frac{r_H(r_H + r_s)}{2r_H + r_s}}. \tag{11}$$

The usual form of BH mass and temperature can be recovered by setting the null density HALO and the null halo radius. The Figs. 1 and 2 show the variations of BH mass surrounded by a DM halo in terms of ρ_s and r_s, respectively.

By satisfying the condition in Eq. (11) and considering $r_s = 0.2$ and $r_H = 1$, we obtain $\rho_s \leq 0.12$.

Figs. 1 and 2 depict the black hole mass as a function of the core density ρ_s and radius r_s, respectively. In Fig. 1, for fixed $r_H = 1$ and $r_s = 0.2$, the mass $M(\rho_s)$ decreases linearly with increasing ρ_s, which indicates that a denser dark halo reduces the black hole mass. This result aligns with the expectation that the presence of an external matter distribution modifies the gravitational potential, effectively reducing the mass parameter of the black hole [42].

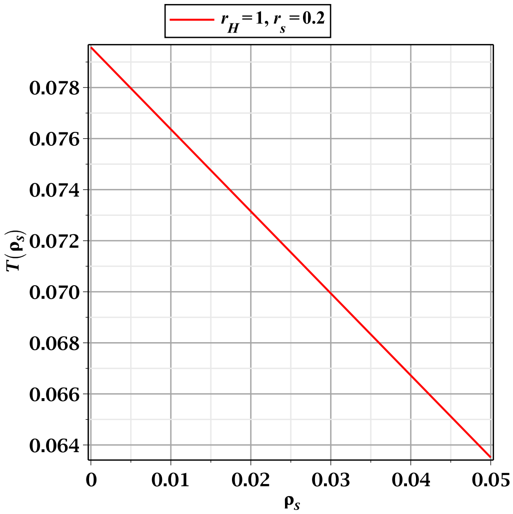

Fig. 3. The impact of central halo density on BH temperature. The other parameters are $r_s = 0.2, r_H = 1$.

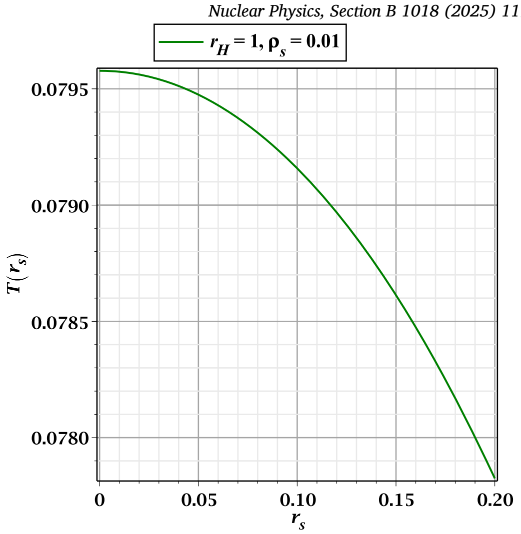

Fig. 4. The impact of central halo radius on BH temperature. The other parameters are $\rho_s = 0.01, r_H = 1$.

Fig. 2 shows the variation of M with r_s for fixed $\rho_s = 0.01$. The mass decreases in a nonlinear fashion as r_s increases. This suggests that an extended halo structure more effectively reduces the black hole mass due to the additional contribution of dark matter at larger scales.

Figs. 3 and 4 illustrate the temperature behavior under the influence of the dark halo. In Fig. 3, we observe that $T(\rho)$ decreases linearly with increasing ρ_s, similar to the behavior of mass. This decline suggests that denser dark halos lead to lower black hole temperatures. While for Fig. 4, one can see that $T(r_s)$ follows a nonlinear decreasing trend, mirroring the mass behavior. This indicates that the halo structure's extension influences the thermodynamic properties of the black hole in a manner consistent with gravitational modifications induced by dark matter. From both Figs. 3 and 4, we conclude that the presence of a DM halo implies a reduced Hawking radiation rate

The other important thermodynamic property is heat capacity because it determines whether the system is locally stable or not, where the negative values indicate local instability, while positive values signify local stability [43]. In the context of BH thermodynamics, it is defined in terms of mass and temperature as follows:

$$C = \frac{dM}{dT} = \frac{dM}{dr_H}\frac{1}{\frac{dT}{dr_H}}, \tag{12}$$

using the obtained expressions for mass and temperature, Eqs. (8) and (10), and by expanding up to the first order of ρ_s, one can easily show that

$$C(r_H) = -2\pi r_H^2\left(1 + \frac{8r_s^4\pi\rho}{r_H^{1/2}(r_H + r_s)^{3/2}}\right). \tag{13}$$

To investigate the effect of the dark halo, we analyze the heat capacity as a function of the core density ρ_s and r_s. The results are presented in Figs. 5 and 6

Fig. 5 depicts the behavior of heat capacity $C(\rho_s)$ for fixed values of $r_H = 1$ and $r_s = 0.2$. The plot shows a linear decrease in C as ρ_s increases while maintaining negative values throughout. The negative heat capacity indicates the well-known instability of asymptotically flat black holes in the canonical ensemble, meaning that energy loss through Hawking radiation leads to further temperature increase rather than stabilization.

Fig. 6 illustrates the variation of heat capacity with the halo radius r_s for a fixed core density $\rho_s = 0.01$. Unlike the linear trend observed for $C(\rho_s)$, $C(r_s)$ exhibits a nonlinear decrease, yet it remains negative throughout. This suggests that while increasing r_s, it still contributes to the black hole's instability.

The additional presence of a dark matter halo does not alter this fundamental instability but enhances the rate at which C decreases, suggesting that denser halos further destabilize the thermodynamic equilibrium of the black hole [44–47].

According to the first law of BH thermodynamics, we have the following relation between entropy, temperature, and mass of BH

$$dS = \frac{dM}{T}. \tag{14}$$

As a result, the entropy of the BH surrounded by the DM halo is given as

$$S(r_H) = \pi r_H^2 \tag{15}$$

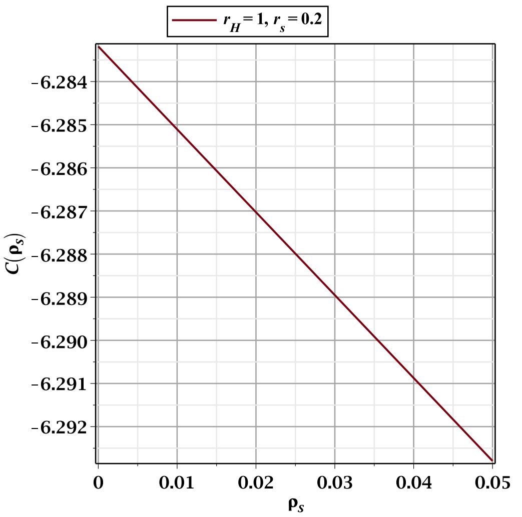

Fig. 5. The impact of central halo density on BH heat capacity. The other parameters are $r_s = 0.2, r_H = 1$.

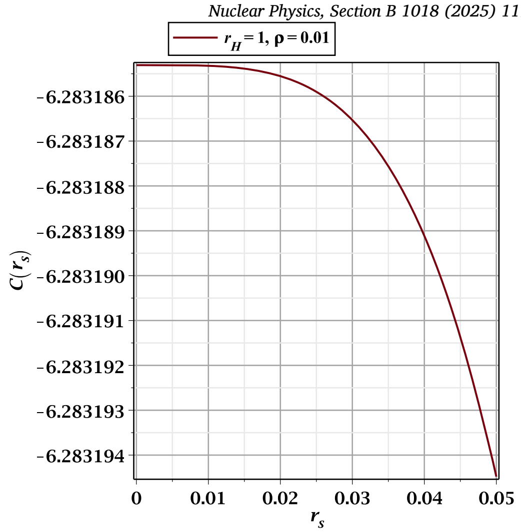

Fig. 6. The impact of central halo radius on BH heat capacity. The other parameters are $\rho_s = 0.01, r_H = 1$.

The presence of the dark matter halo could in principle, modify the entropy due to alterations in the surrounding gravitational field [39,48]. However, our calculations reveal an interesting result: the correction due to the dark halo does not affect the entropy formula, and it remains identical to that of an isolated Schwarzschild black hole.

This finding has significant implications for black hole thermodynamics in dark matter environments:

- The entropy of a black hole remains a robust quantity, unaffected by the presence of a surrounding dark matter halo.
- This result may indicate that while dark matter modifies other thermodynamic properties such as mass, temperature, and heat capacity, it does not interfere with the fundamental statistical mechanical interpretation of black hole entropy.

Calculating the Gibbs free energy function is crucial to determine whether the studied black hole system is globally stable. Negative values indicate global stability, while positive values indicate instability [43]. The Gibbs free energy function is related to mass, temperature, and entropy through the following relation:

$$G(r_H) = M(r_H) - T(r_H)S(r_H), \tag{16}$$

using the expressions (8), (10) and (15), the expression of $G(r_H)$, up to the first order of ρ_s, is written as

$$G(r_H) = \frac{r_H}{4} + \rho_s \mathcal{G}(r_H), \tag{17}$$

where $\mathcal{G}(r_H)$ is given as

$$\mathcal{G}(r_H) = 16\pi r_s^2 \left[\frac{(2r_H + r_s)}{\sqrt{r_H(r_H + r_s)}} - 4\sqrt{1 + \frac{r_s}{r_H}} \right]. \tag{18}$$

To show the impact of ρ_s and r_s, we plotted the Figs. 7 and 8

Our results show that the Gibbs free energy decreases linearly as a function of ρ_s, as illustrated in Fig. 7. This behavior suggests that as the core density of the halo increases, the black hole's thermodynamic potential reduces predictably. The linearity implies that the contribution of the dark matter halo to the free energy follows a straightforward scaling law, where denser halos lead to a proportionally greater reduction in G. In contrast, the variation of G with r_s exhibits a nonlinear decreasing trend, as shown in Fig. 8. Both figures show that the presence of a DM halo makes the BH globally less unstable.

Let us now examine whether phase transitions occur in the context of our study. To determine this, it is essential to plot the Gibbs free energy as a function of temperature for various selected values of ρ_s and r_s.

We can observe from the Fig. 9 that the Gibbs free energy decreases more rapidly as the influence of the dark matter halo increases. Moreover, since there are no two distinct values of the Gibbs free energy corresponding to the same temperature, this implies that no phase transition occurs.

At the end of this section, it is important to note that the obtained lapse function and therefore the thermodynamic properties exhibit novel features that distinguish it from well-known models such as the Bardeen black hole, however, we would like to emphasize that it reduces to the standard Schwarzschild black hole in the appropriate limiting cases, which are $r_s \to 0$, or $\rho_s \to 0$ (absence of DM halo).

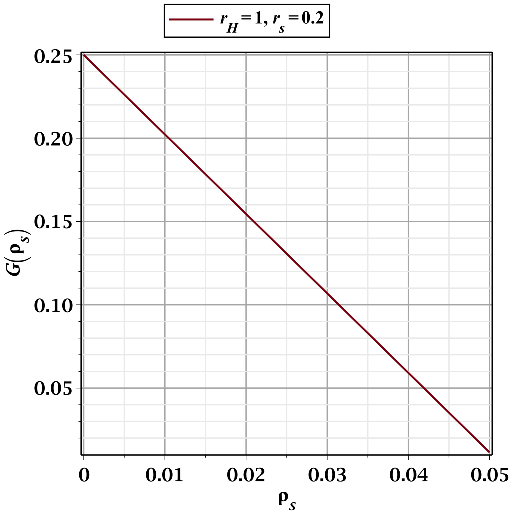

Fig. 7. The impact of central halo density on BH Gibbs free energy. The other parameters are $r_s = 0.2, r_H = 1$.

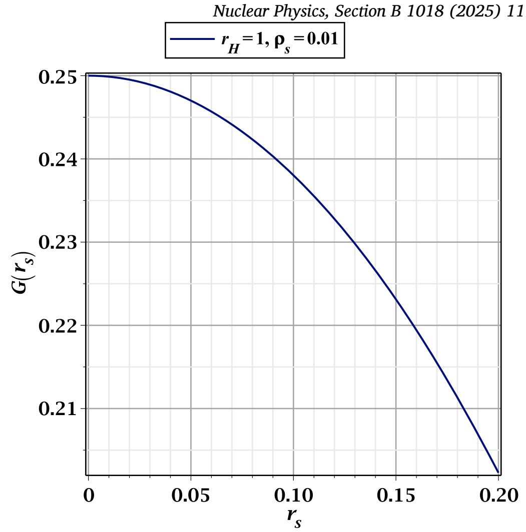

Fig. 8. The impact of central halo radius on BH Gibbs free energy. The other parameters are $\rho_s = 0.01, r_H = 1$.

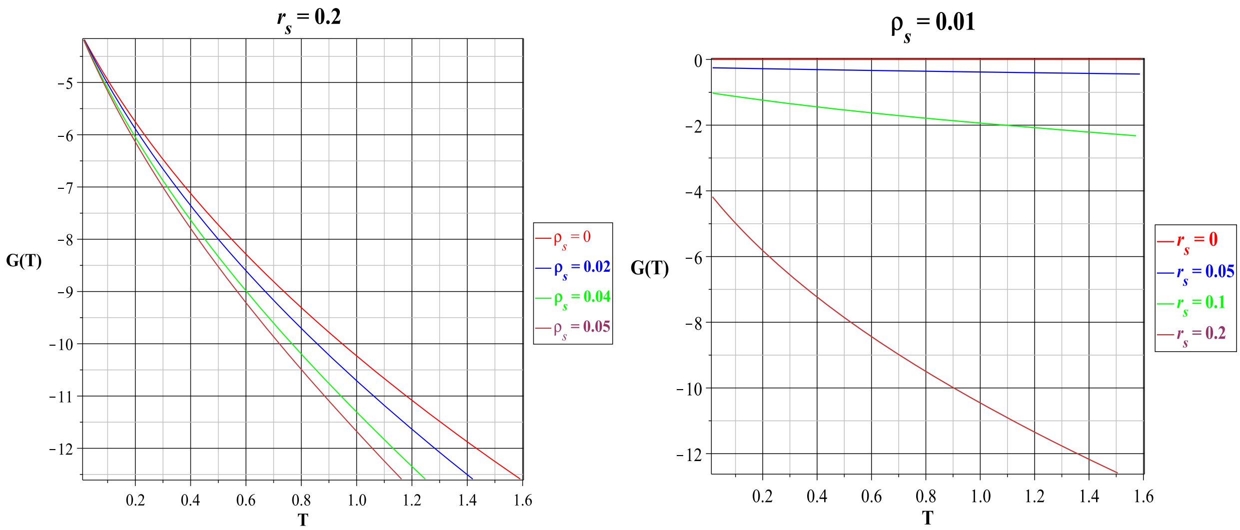

Fig. 9. The effect of central halo density and radius on the variation of Gibbs free energy with temperature T.

In the following, we will study how the presence of a dark matter (DM) halo influences the circular motion of massless particles, such as photons.

3. Photon circular orbit radius

Studying photon trajectories around black holes provides crucial insights into the underlying spacetime geometry and observational signatures such as shadow and gravitational lensing effects [49–51]. In particular, the photon circular orbit radius is fundamental in determining the innermost stable paths that light can follow around a black hole [52]. This is governed by the effective potential, which depends on the spacetime metric components and encapsulates the gravitational influence exerted by the black hole and its surrounding environment [53].

In the standard method, the circular photon orbit is determined by identifying the critical points of the effective potential V_{eff}. Where we will now prove its general relation in terms of the lapse function. For photons, we have the following constraint (null geodesic):

$$-f(r)\dot{t}^2 + \frac{1}{f(r)}\dot{r}^2 + r^2\left(\dot{\theta}^2 + \sin^2(\theta)\dot{\phi}^2\right) = 0, \quad (19)$$

on the other hand, the Lagrangian of the system is:

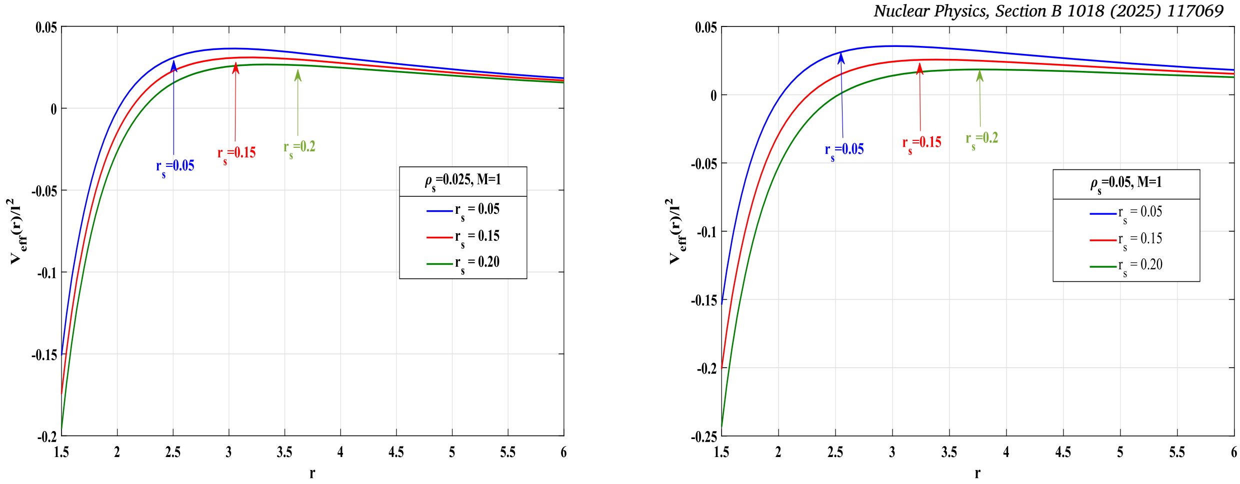

Fig. 10. The impact of central halo radius on the variation of the effective potential as a function of r. The other parameters are $\rho_s = 0.025$, $\rho_s = 0.05$ and $M = 1$.

$$L = \frac{1}{2} g_{\mu\nu} \dot{x}^\mu \dot{x}^\nu, \tag{20}$$

where $\dot{x}^\mu = \frac{dx^\mu}{d\tau}$, and τ is any affine parameter of null geodesics. By applying the Euler-Lagrange equations to the Lagrangian (20), one can readily demonstrate that the following quantities are conserved.

$$E = -\frac{1}{2}\frac{\partial L}{\partial \dot{t}} = f(r)\dot{t}, \tag{21}$$

$$l = -\frac{1}{2}\frac{\partial L}{\partial \dot{\phi}} = r^2 \sin^2(\theta)\dot{\phi}. \tag{22}$$

E and l are the energy and angular momentum, respectively. If we restrict test particles moving in the equatorial plane, $\theta = \pi/2$, the null geodesic equation (19) eventually reduces to:

$$E^2 = \dot{r}^2 + V_{\rm eff}(r), \tag{23}$$

where the effective potential $V_{\rm eff}$ of the photon is related to the lapse function $f(r)$ as follows

$$V_{\rm eff}(r) = \frac{l^2 f(r)}{r^2}. \tag{24}$$

In the studied system, the lapse function is given in Eq. (7), therefore

$$V_{\rm eff}(r) = \frac{l^2}{r^2}\left[1 - \frac{2M}{r} - 32\pi\rho_s r_s^3 \sqrt{\frac{r+r_s}{r_s^2 r}}\right]. \tag{25}$$

As demonstrated in the previous sections, dark matter halo modifies the lapse function $f(r)$ introducing deviations from the standard Schwarzschild. These modifications, in turn, affect the structure of the effective potential Eq. (25). Notably, the additional term introduced by the dark matter halo is negative, leading to a reduction in the effective potential for all values of r, r_s, and ρ_s. It is important to note that the study of the effect of the DM halo using the Dehnen-type profile has been conducted for massive particles [23].

To assess the stability of the photon circular orbit, we analyze the behavior of the effective potential $V_{eff}(r)$. As depicted in Figs. 10 and 11, the potential exhibits a characteristic profile: it initially increases from negative values, crosses zero, and reaches a local maximum before gradually decreasing toward zero at infinity. One can also observe that the effective potential increases, including its maximum value, as the core halo density decreases. The existence of only maximum values indicates that the circular trajectory of the photon (whose radius corresponds to the maximum value of $V_{\rm eff}$) is unstable.

The photon orbit occurs at the peak of $V_{eff}(r)$, where the second derivative of the effective potential is negative $V''_{eff}(r) < 0$, confirming that the orbit is unstable. This result aligns with general relativistic predictions that photon circular orbits around black holes are inherently unstable, meaning that any small perturbation will cause the photon to either spiral inward toward the event horizon or escape to infinity.

The circular photon orbit, also known as the photon sphere, exists at a radius $r = r_c$ when the following condition is satisfied,

$$\frac{dV_{eff}(r)}{dr}\Big|_{r=r_c} = 0, \tag{26}$$

this ensures that the force acting on the photon vanishes at $r = r_c$, meaning the orbit is stationary.

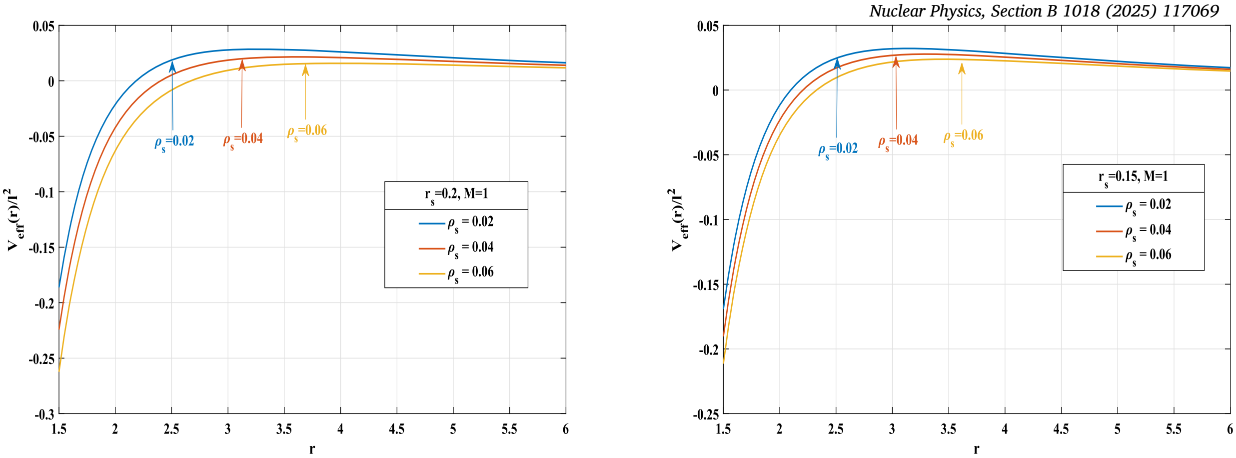

Fig. 11. The impact of central halo density on the variation of the effective potential as a function of r. The other parameters are $r_s = 0.15$, $r_s = 0.2$ and $M = 1$.

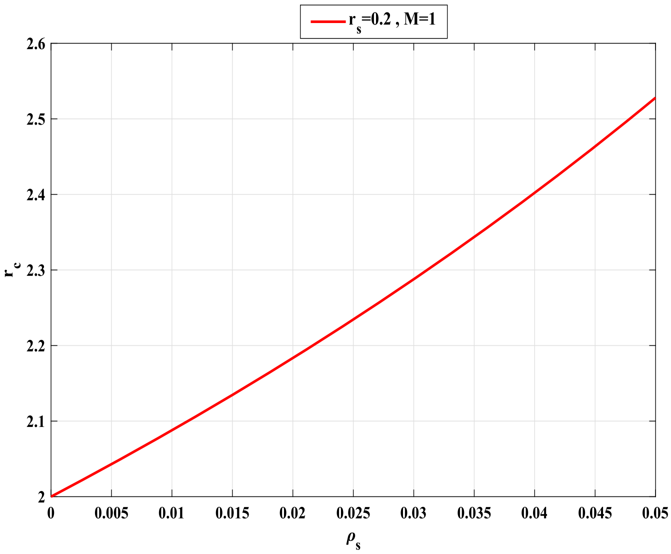

Fig. 12. The variations of the photon sphere radius r_c as a function of central halo density ρ_s for fixed $r_s = 0.2$ and $M = 1$.

Given the complexity of the analytical solution and in order to find the effects of ρ_s and r_s on the radius of the circular orbit for photon, we plotted directly the variations of r_c as a function of central halo density (ρ_s) in Fig. 12 and radius (r_s) in Fig. 13.

Fig. 13 presents the variation of r_c as a function of the core density ρ_s for a fixed characteristic radius $r_s = 0.2$. The observed trend reveals a monotonic increase in r_c with increasing ρ_s, indicating that denser halos have a stronger influence on the photon orbit. This suggests that the concentration of dark matter near the black hole plays a significant role in shaping the photon capture region.

Fig. 12 illustrates the dependence of the photon sphere radius r_c on the characteristic radius for a fixed halo density $\rho_s = 0.01$. The results indicate that as r_s increases, the photon sphere radius increases non-linearly. This suggests that a more extended dark matter halo enhances the gravitational lensing effects by shifting the photon orbit further outward.

4. BH shadow and energy emission rate

4.1. BH shadow

The critical impact parameter b_c defines the threshold for photon capture by a black hole; photons with $b > b_c$ escape to infinity, while those with $b \leq b_c$ are absorbed, forming the observable boundary of the black hole shadow [54]. It corresponds to unstable circular photon orbits, known as the *photon sphere* [55]. Mathematically, b_c is written in terms of unstable circular photon radius as follows [56],

$$b_c = \frac{L}{E} = \frac{r_c}{\sqrt{f(r_c)}}. \tag{27}$$

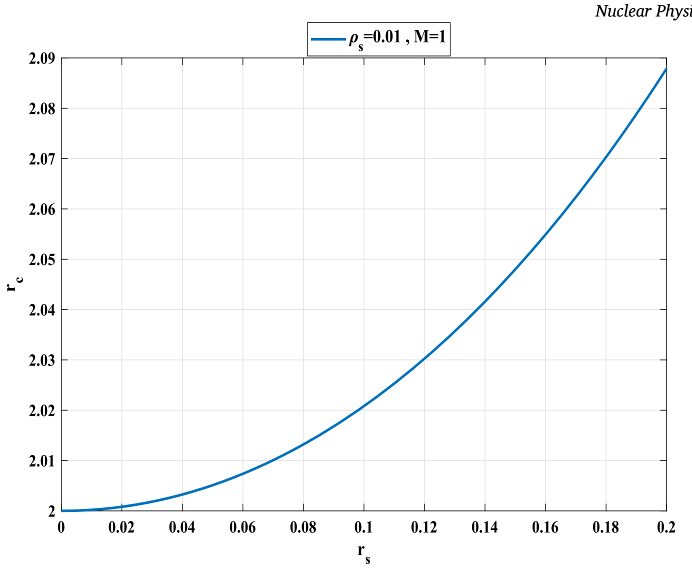

Fig. 13. The variations of the photon sphere radius r_c as a function of core radius r_s for fixed $\rho_s = 0.01$ and $M = 1$.

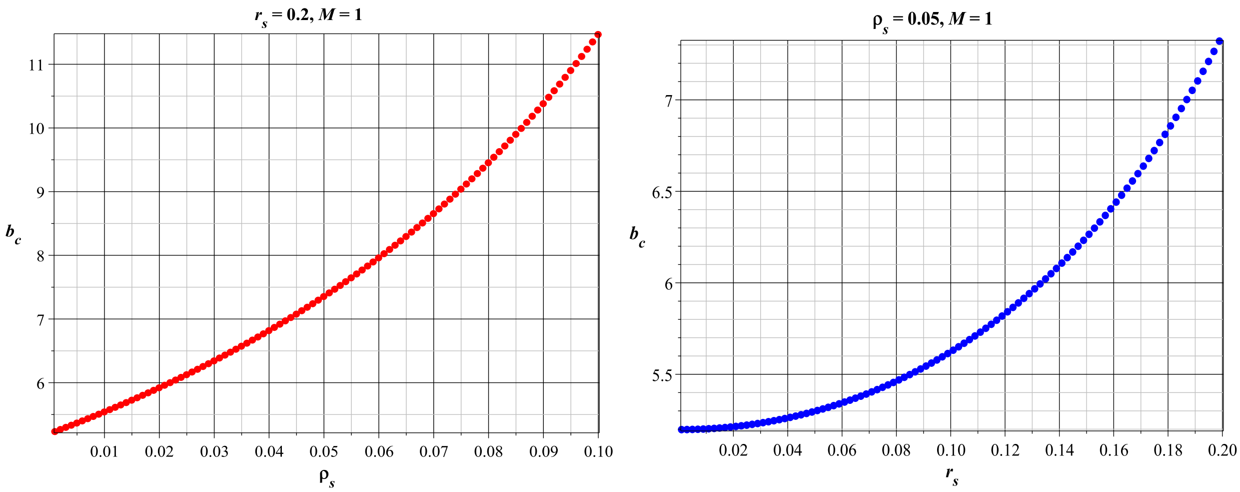

Fig. 14. The effect of central halo density and radius on the critical impact parameter.

On the other hand, the BH shadow refers to the dark region observed against a luminous background, caused by extreme gravitational lensing near the event horizon. It corresponds to the apparent boundary of photon capture, determined by unstable photon orbits. The radius of the BH shadow is given as

$$r_{SH} = \frac{r_c}{\sqrt{f(r_c)}}\sqrt{f(r_0)}, \tag{28}$$

here, r_0 denotes the observer's distance. Therefore, if r_0 is fixed, the behavior of the black hole shadow radius and the critical impact parameter are identical.

To show how the DM halo affects the critical impact parameter, and therefore the BH shadow radius, we present how it changes with central halo density and radius in Fig. 14.

We observe that increasing both the central halo density ρ_s and the halo radius r_s leads to an increase in the critical impact parameter b_c, and thus in the black hole shadow radius R_{sh}.

4.2. Energy emission rate

Quantum fluctuations in the black hole spacetime lead to the spontaneous creation and annihilation of particle-antiparticle pairs near the event horizon. In this context, particles with positive energy can escape via quantum tunneling, giving rise to Hawking radiation. This phenomenon results in the gradual evaporation of the black hole over a finite timescale. In this subsection, we analyze

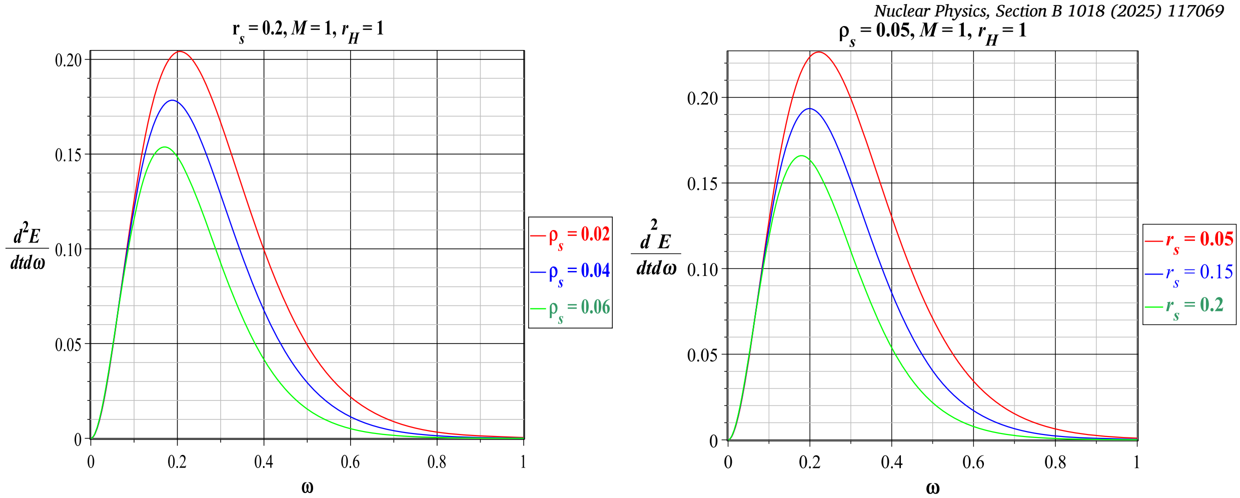

Fig. 15. The effect of central halo density and radius on the Energy emission rate.

the corresponding energy emission rate. One can extract the energy emission rate starting from BH shadow radius, and Hawking temperature T_H by the following expression [57],

$$\frac{d^2E}{d\omega\, dt} = \frac{2\pi^3 r_{\rm SH}\omega^3}{\exp\left(\frac{\omega}{T_H}\right) - 1}. \tag{29}$$

Here, ω denotes the frequency of the emitted photon, and $r_{\rm SH}$ represents the radius of the black hole (BH) shadow, which corresponds to the projection of the BH's unstable photon orbit onto the observer's sky, which is given in terms of the unstable orbit radius r_c in Eq. (28). The Hawking temperature T_H in terms of ρ_s and r_s is written in Eq. (10).

To examine the influence of the dark matter (DM) halo parameters ρ_s and r_s on the energy emission rate, we subsequently present this rate as a function of the emitted photon frequency for various values of these parameters in Fig. 15.

It can be observed that the energy emission rate increases under the influence of the dark matter halo at sufficiently low frequencies. However, as the frequency increases, this trend reverses, and the presence of dark matter leads to a suppression of the emission rate. Furthermore, the frequency corresponding to the peak of the energy emission rate decreases as the influence of the dark matter halo becomes more pronounced.

At the end of this paper, it should be noted that the key difference between reference [39] and our work is that the former assumes $\gamma = 0$ for the Dehnen dark matter distribution, while in our study we consider $\gamma = \frac{5}{2}$. Furthermore, reference [39] does not investigate the effect of r_s on the thermodynamic properties, the photon trajectories, or the black hole shadow radius. Moreover, the authors of the same reference did not address the impact of dark matter media on the critical impact parameter b_c nor on the energy emission rate. Additionally, we show that the effective potential for photons around the studied black hole always increases with increasing ρ_s, regardless of the value of r; this behavior is not reported in Ref. [39].

5. Conclusion

We have studied the effect of a dark matter (DM) halo on the thermodynamic properties of Schwarzschild black holes, incorporating the Dehnen-type profile. Our findings indicate that the presence of a DM halo significantly influences black hole mass, temperature, heat capacity, entropy, Gibbs free energy, and radius of the circular motion of photons around the black hole. In particular, mass, temperature, heat capacity, and Gibbs free energy decrease in the presence of dark matter, with a linear dependence on the core density ρ_s and a nonlinear dependence on the halo radius r_s. Remarkably, the black hole entropy remains unchanged, retaining the standard Bekenstein-Hawking formula $S = \pi^2 r_H$, which suggests that the presence of dark matter does not alter the fundamental entropy-area relation. As a physical interpretation of these results, the presence of a DM halo effectively reduces the evaporation rate of black holes by lowering their temperature; additionally, it decreases both global and local instability, while the number of degrees of freedom carried by the black hole surface remains unaffected by the DM halo.

On the other hand, the presence of the dark matter (DM) halo leads to an increase in the radius of circular motion, as well as an enhancement in both the critical impact parameter and the black hole shadow radius. Moreover, we observed that the energy emission rate decreases under the influence of the DM halo at sufficiently low frequencies. However, as the frequency increases, this trend reverses. It is also noteworthy that the frequency corresponding to the peak emission shifts to lower values as the influence of the DM halo becomes more significant.

These findings underscore the significant role of dark matter in modifying black hole thermodynamics while preserving the entropy law. This study provides valuable insights into the behavior of black holes in astrophysical dark matter environments, with potential implications for both observational and theoretical research.

CRediT authorship contribution statement

Abdelhakim Benkrane: Conceptualization, Investigation, Methodology, Project administration, Writing – original draft, Writing – review & editing. **Djamel Eddine Zenkhri:** Conceptualization, Investigation, Methodology, Writing – original draft, Visualization, Writing – review & editing.

Declaration of competing interest

The authors declare that they have no known competing financial interests or personal relationships that could have appeared to influence the work reported in this paper.

Acknowledgements

We would like to express my sincere gratitude to the reviewers for their valuable comments and constructive suggestions, which have greatly contributed to improving the quality and clarity of this manuscript.

Data availability

No data was used for the research described in the article.

References

[1] Martin J. Rees, Black hole models for active galactic nuclei, Annu. Rev. Astron. Astrophys. 22 (1984) 471–506.
[2] John Kormendy, Douglas Richstone, Inward bound—the search for supermassive black holes in galactic nuclei, Annu. Rev. Astron. Astrophys. 33 (1995) 581.
[3] Gianfranco Bertone, Tim M.P. Tait, A new era in the search for dark matter, Nature 562 (7725) (2018) 51–56.
[4] Vera C. Rubin, W. Kent Ford Jr., Rotation of the Andromeda nebula from a spectroscopic survey of emission regions, Astrophys. J. 159 (1970) 379.
[5] Edvige Corbelli, Paolo Salucci, The extended rotation curve and the dark matter halo of m33, Mon. Not. R. Astron. Soc. 311 (2) (2000) 441–447.
[6] Eiichiro Komatsu, J. Dunkley, M.R. Nolta, C.L. Bennett, B. Gold, G. Hinshaw, N. Jarosik, D. Larson, M. Limon, L.E.A. Page, et al., Five-year Wilkinson microwave anisotropy probe* observations: cosmological interpretation, Astrophys. J. Suppl. Ser. 180 (2) (2009) 330.
[7] Yi Yang, Dong Liu, Ali Övgün, Gaetano Lambiase, Zheng-Wen Long, Black hole surrounded by the pseudo-isothermal dark matter halo, Eur. Phys. J. C 84 (1) (2024) 1–14.
[8] Ming-Hsun Li, Kwei-Chou Yang, Galactic dark matter in the phantom field, Phys. Rev. D, Part. Fields Grav. Cosmol. 86 (12) (2012) 123015.
[9] Seyed Hossein Hendi, Azadeh Nemati, Kai Lin, Jamil Mubasher, Instability and phase transitions of a rotating black hole in the presence of perfect fluid dark matter, Eur. Phys. J. C 80 (2020) 1–12.
[10] Muhammad Rizwan, Mubasher Jamil, Kimet Jusufi, Distinguishing a Kerr-like black hole and a naked singularity in perfect fluid dark matter via precession frequencies, Phys. Rev. D 99 (2) (2019) 024050.
[11] Sanjar Shaymatov, Bobomurat Ahmedov, Jamil Mubasher, Testing the weak cosmic censorship conjecture for a Reissner–Nordström–de Sitter black hole surrounded by perfect fluid dark matter, Eur. Phys. J. C 81 (2021) 1–11.
[12] Javlon Rayimbaev, Sanjar Shaymatov, Jamil Mubasher, Dynamics and epicyclic motions of particles around the Schwarzschild–de Sitter black hole in perfect fluid dark matter, Eur. Phys. J. C 81 (2021) 1–12.
[13] Sanjar Shaymatov, Daniele Malafarina, Bobomurat Ahmedov, Effect of perfect fluid dark matter on particle motion around a static black hole immersed in an external magnetic field, Phys. Dark Universe 34 (2021) 100891.
[14] Vitor Cardoso, Kyriakos Destounis, Francisco Duque, Rodrigo Panosso Macedo, Andrea Maselli, Black holes in galaxies: environmental impact on gravitational-wave generation and propagation, Phys. Rev. D 105 (6) (2022) L061501.
[15] Xian Hou, Zhaoyi Xu, Ming Zhou, Jiancheng Wang, Black hole shadow of sgr a* in dark matter halo, J. Cosmol. Astropart. Phys. 2018 (07) (2018) 015.
[16] Zibo Shen, Anzhong Wang, Yungui Gong, Shaoyu Yin, Analytical models of supermassive black holes in galaxies surrounded by dark matter halos, Phys. Lett. B (2024) 138797.
[17] D. Blas, D.L. Nacir, S. Sibiryakov, The structure of cold dark matter halos, Astrophys. J. 462 (1996) 563.
[18] Aaron A. Dutton, Andrea V. Maccio, Cold dark matter haloes in the Planck era: evolution of structural parameters for einasto and nfw profiles, Mon. Not. R. Astron. Soc. 441 (4) (2014) 3359–3374.
[19] David Merritt, Alister W. Graham, Ben Moore, Juerg Diemand, Balša Terzić, Empirical models for dark matter halos. i. Nonparametric construction of density profiles and comparison with parametric models, Astron. J. 132 (6) (2006) 2685.
[20] Andreas Burkert, The structure of dark matter halos in dwarf galaxies, Astrophys. J. 447 (1) (1995) L25.
[21] Walter Dehnen, A family of potential–density pairs for spherical galaxies and bulges, Mon. Not. R. Astron. Soc. 265 (1) (1993) 250–256.
[22] B. Shukirgaliyev, A. Otebay, M. Sobolenko, M. Ishchenko, O. Borodina, T. Panamarev, S. Myrzakul, M. Kalambay, A. Naurzbayeva, E. Abdikamalov, et al., Bound mass of Dehnen models with a centrally peaked star formation efficiency, Astron. Astrophys. 654 (2021) A53.
[23] Ahmad Al-Badawi, Sanjar Shaymatov, Yassine Sekhmani, Schwarzschild black hole in galaxies surrounded by a dark matter halo, J. Cosmol. Astropart. Phys. 2025 (02) (2025) 014.
[24] Jacob D. Bekenstein, Black holes and entropy, Phys. Rev. D 7 (8) (1973) 2333.
[25] Jacob D. Bekenstein, Statistical black-hole thermodynamics, Phys. Rev. D 12 (10) (1975) 3077.
[26] Stephen W. Hawking, Black hole explosions?, Nature 248 (5443) (1974) 30–31.
[27] Stephen W. Hawking, Particle creation by black holes, Commun. Math. Phys. 43 (3) (1975) 199–220.
[28] James M. Bardeen, Brandon Carter, Stephen W. Hawking, The four laws of black hole mechanics, Commun. Math. Phys. 31 (1973) 161–170.
[29] B. Carter, Properties of the Kerr Metric, DeWitt and DeWitt, 1973.
[30] Jacob D. Bekenstein, Generalized second law of thermodynamics in black-hole physics, Phys. Rev. D 9 (12) (1974) 3292.
[31] Erik Verlinde, On the origin of gravity and the laws of Newton, J. High Energy Phys. 2011 (4) (2011) 29.
[32] Kamel Ourabah, The other way around: from alternative gravity to entropy, Class. Quantum Gravity 41 (1) (2023) 015010.
[33] Ahmad Sheykhi, Seyed Hossein Hendi, Power-law entropic corrections to Newton's law and Friedmann equations, Phys. Rev. D, Part. Fields Grav. Cosmol. 84 (4) (2011) 044023.
[34] Piero Nicolini, Entropic force, noncommutative gravity, and ungravity, Phys. Rev. D, Part. Fields Grav. Cosmol. 82 (4) (2010) 044030.

[35] H. Moradpour, A. Sheykhi, C. Corda, Ines G. Salako, Implications of the generalized entropy formalisms on the Newtonian gravity and dynamics, Phys. Lett. B 783 (2018) 82–85.
[36] Archil Kobakhidze, Gravity is not an entropic force, Phys. Rev. D, Part. Fields Grav. Cosmol. 83 (2) (2011) 021502.
[37] Spyros Basilakos, Joan Sola, Entropic-force dark energy reconsidered, Phys. Rev. D 90 (2) (2014) 023008.
[38] Houjun Mo, Frank Van den Bosch, Simon White, Galaxy Formation and Evolution, Cambridge University Press, 2010.
[39] Mrinnoy M. Gohain, Prabwal Phukon, Kalyan Bhuyan, Thermodynamics and null geodesics of a Schwarzschild black hole surrounded by a Dehnen type dark matter halo, Phys. Dark Universe 46 (2024) 101683.
[40] Scott Tremaine, Douglas O. Richstone, Yong-Ik Byun, Alan Dressler, S.M. Faber, Carl Grillmair, John Kormendy, Tod R. Lauer, A family of models for spherical stellar systems, Astron. J. (ISSN 0004-6256) 107 (2) (1994) 634–644.
[41] Reggie C. Pantig, Ali Övgün, Dehnen halo effect on a black hole in an ultra-faint dwarf galaxy, J. Cosmol. Astropart. Phys. 2022 (08) (2022) 056.
[42] Yifeng Zhou, Jiaxin Han, A physical and concise halo model based on the depletion radius, Mon. Not. R. Astron. Soc. 525 (2) (2023) 2489–2508.
[43] Abdelhakim Benkrane, Djamel Eddine Zenkhri, Abderrahmane Benhadjira, Effects of the new type of extended uncertainty principle on van der Waals black hole thermodynamics: a theoretical and deep learning approach, Mod. Phys. Lett. A 39 (10) (2024) 2450041.
[44] R. Silva, J.S. Alcaniz, Negative heat capacity and non-extensive kinetic theory, Phys. Lett. A 313 (5–6) (2003) 393–396.
[45] Zacharias Roupas, Gravitational instability caused by the weight of heat, Symmetry 11 (12) (2019) 1435.
[46] Swastik Bhattacharya, S. Shankaranarayanan, Negative specific heat of black-holes from fluid-gravity correspondence, Class. Quantum Gravity 34 (7) (2017) 075005.
[47] Adi Nusser, Gravo-thermodynamics of the intracluster medium: negative heat capacity and dilation of cooling time scales, New Astron. 14 (4) (2009) 365–368.
[48] Reggie C. Pantig, Apparent and emergent dark matter around a Schwarzschild black hole, Phys. Dark Universe 45 (2024) 101550.
[49] Akash K. Mishra, Sumanta Chakraborty, Sudipta Sarkar, Understanding photon sphere and black hole shadow in dynamically evolving spacetimes, Phys. Rev. D 99 (10) (2019) 104080.
[50] Pedro V.P. Cunha, Carlos A.R. Herdeiro, Shadows and strong gravitational lensing: a brief review, Gen. Relativ. Gravit. 50 (2018) 1–27.
[51] Yiyang Wang, Amnish Vachher, Qiang Wu, Tao Zhu, Sushant G. Ghosh, Strong gravitational lensing by static black holes in effective quantum gravity, Eur. Phys. J. C 85 (3) (2025) 1–18.
[52] Hyun-Chul Lee, Yong-Jin Han, Innermost stable circular orbit of Kerr-mog black hole, Eur. Phys. J. C 77 (2017) 1–9.
[53] Chen-Kai Qiao, Ming Li, Geometric approach to circular photon orbits and black hole shadows, Phys. Rev. D 106 (2) (2022) L021501.
[54] S. Chandrasekhar, The Mathematical Theory of Black Holes, Oxford University Press, 1983.
[55] J.M. Bardeen, Timelike and null geodesics in the Kerr metric, in: C. DeWitt, B. DeWitt (Eds.), Black Holes, Les Houches, 1972, Gordon and Breach, 1973, pp. 215–239.
[56] V. Perlick, O.Y. Tsupko, G.S. Bisnovatyi-Kogan, Black hole shadow in an expanding universe with a cosmological constant, Phys. Rev. D 97 (10) (2018) 104062.
[57] Ghulam Mustafa, Farruh Atamurotov, Ibrar Hussain, Sanjar Shaymatov, Ali Övgün, Shadows and gravitational weak lensing by the Schwarzschild black hole in the string cloud background with quintessential field, Chin. Phys. C 46 (12) (2022) 125107.